

Laser-GMA Hybrid Welding: Process Monitoring and Thermal Modeling

E.W. Reutzel, S.M. Kelly, R.P. Martukanitz

Applied Research Laboratory, Pennsylvania State University, State College, PA, USA

M.M. Bugarewicz, P. Michaleris

Dept. of Mechanical and Nuclear Engineering, Pennsylvania State University, University Park, PA, USA

Abstract

Laser-Gas Metal Arc (GMA) hybrid welding is an increasingly accepted technology for a variety of commercial applications, from industries as diverse as shipbuilding to automobile manufacture. As applications become more widespread, there is a growing need to understand the relationship between the numerous process parameters and the process results, including weld quality and distortion. To build upon the body of knowledge supporting this, two separate experiments are performed.

In the first, hybrid welds are performed with a 2.6 kW Nd:YAG laser and sensors are used to monitor GMA voltage and current, as well as the arc-plasma electromagnetic emissions in both the ultraviolet and infrared regions. Process perturbations, such as fluctuations in GMAW voltage and wire speed, laser angle of incidence, and laser/GMAW torch head separation distance, are introduced to study their effect on sensor output.

Finally, thermal finite element models are developed and used to quantify the varying heat input per unit length when compared with conventional GMAW and laser welding processes, particularly as applied to joining of thin steel structures. The onset of buckling during weld fabrication has been shown to be strongly dependent upon the heat input used to produce the weld. A thermal model of the laser-GMA hybrid welding process is developed to serve as a representation of this complex process.

Introduction

It has been nearly a quarter of a century since researchers first conceived of combining a conventional welding arc with a laser beam in a hybrid process [1, 2], but only recently has laser-GMA hybrid welding begun to be utilized in industrial applications.

Laser beam welding offers relatively high welding speed compared to conventional processes and high penetration that is achieved due to the keyhole effect. Unfortunately, due to the small spot size of the laser, it has limited success

in some welding applications because of insufficient gap bridging capabilities, requiring high precision during edge preparation and setup. Additionally, the focussed energy of the laser beam results in a narrow heat affected zone (HAZ) that can lead to steep spatial and temporal thermal gradients that sometimes result in brittle microstructures.

In contrast, conventional GMAW offers the ability to easily bridge gaps in the joint by introducing filler metal to the process. The composition of the filler materials can be customized to produce improved material properties. The additional heat results in reduced cooling rates, often leading to improved ductility. However, the high heat can result in undesirable distortion or buckling, and the physics of the process result in an inability to produce deep penetration welds. As a result, thick sections are often welded with multiple weld passes.

These shortcomings can be overcome by combining the laser with an arc welding technique such as GMAW. Not only is this helpful in accommodating gaps and reducing weld-head positioner tolerance requirements while maintaining deep penetration [3], but it has also been known to produce even greater welding speeds and to provide an improved weld microstructure upon cooling [4].

This document outlines recent results of various investigations into both practical and theoretical aspects of laser-GMA hybrid welding. The first section discusses how various sensors can provide information regarding the state of the hybrid welding process. The next section presents results of experiments to introduce a single-pass hybrid weld as a substitute for a multi-pass conventional weld for thick substrates. The final section discusses initial attempts to define a theoretical thermal model of the hybrid welding process that will be used to quantify distortion and buckling for comparison of the laser, gas metal arc, and hybrid welding processes.

Process Monitoring

Detection of weld defects using real time monitoring methods is of significant concern in industry. This is

largely due to the increased production and liability costs that result when weld defects are not identified early in the production cycle. Weld monitoring systems must be reliable, flexible and cost effective in non-clean, high-volume production environments. Various sensors in the field of real time weld monitoring have shown promise in detecting weld process conditions. These include acoustic, plasma-based, optical (infrared, ultraviolet and x-ray) and electromagnetic sensors. In the laser welding process alone, the range of signal emissions from the weld zone has led to a wide range of techniques being applied to sensing of the process [5, 6, 7]. In conventional arc welding, parameters such as voltage and current have been monitored to determine characteristics and health of the weld process [8, 9].

When the laser welding process is combined with conventional GMAW, it is clear that the processes will interact and necessarily affect one another (See Figure 1). With a constant voltage welding power supply, the resistance of the wire stick-out and arc are inversely proportional to the output current of the power supply. It is reasonable to expect that the additional heat deposited by the laser beam, and the additional metal vapor and ions that are expelled from the keyhole during welding will affect the arc resistance, and therefore the arc current. It is relatively simple to measure the arc current using a Hall-effect probe, and experiments revealed that the arc current correlates closely with changes in many process variables. It is believed monitoring of this single parameter could enable determination of a variety of process variables that are difficult to monitor otherwise. A few examples are discussed below.

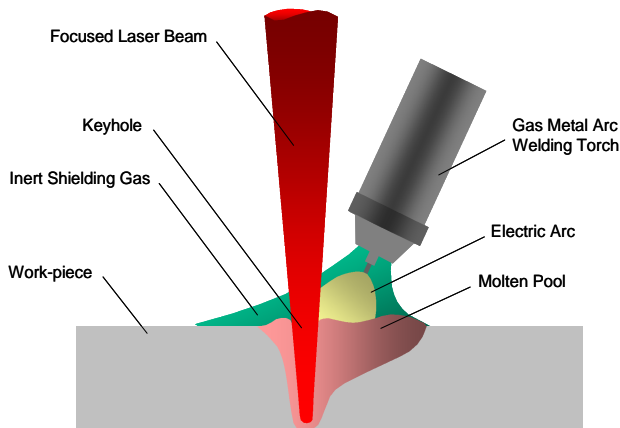


Figure 1: Schematic of the hybrid welding process.

Affect of laser on arc current

To investigate the affect of laser on the arc current, a hybrid laser-GMA bead-on-plate weld was performed, and the laser was terminated halfway through the weld length, in order

to observe variations in sensor output. A variety of different voltage set-points were tested. The arc currents obtained during these experiments are shown in Figure 2. For a given wire feed speed (WFS), at lower voltages there was a dramatic increase in current when the laser was removed from the system. At 18 V it can be seen that there is an increase in current of approximately 30 A upon deactivation of the laser. In all cases, WFS was 76 mm/s (180 ipm), gas (Ar-25% O₂) flow rate was 35 CFH, and the laser was applied for the first half of the weld, then deactivated for the second half. With increasing arc voltage, these effects became much less pronounced.

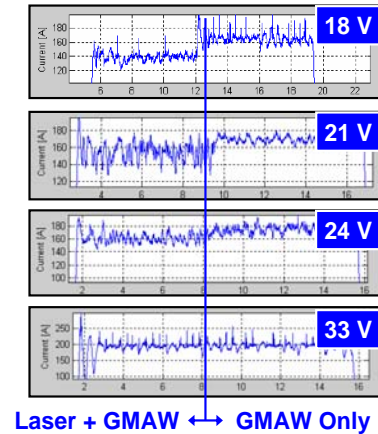


Figure 2: Affect of laser at different voltage set-points on arc current.

A possible explanation for this behavior can be developed by considering that as arc length increases, resistance also increases since the electrons have a greater distance to travel. An increase in arc length can be caused by increasing penetration depth, therefore the value of the current can be strongly correlated to penetration. The constant voltage power supply used during the experiments exhibits a positive slope for the voltage and current characteristics in order to maintain Ohm's Law, $V = IR$ (where V is voltage, I is current, and R is resistance). Therefore, penetration and welding current are directly proportional. As penetration decreases when the laser is deactivated, the arc length is reduced and current must increase.

In GMA welding, the penetration has been shown to increase as the voltage is increased. At lower voltage set-points, such as 18 V, the difference between the penetration of the hybrid and the GMAW process is more pronounced. This could explain the relatively large increase in current when deactivating the laser. As voltage is increased and arc force increases, one can expect less of a difference in penetration when the laser is deactivated and therefore a smaller increase in current. However, other hybrid experiments involving an increase of laser power, and therefore penetration, did not demonstrate this same

decrease in current, and therefore raises questions with this theory. Other explanations are discussed in Travis *et al* [10, 11].

Affect of laser-to-arc spacing on arc current

It has been reported that varying the laser position relative to the GMAW torch affects the welding process [12, 13]. To evaluate this effect, this distance was varied using 22 V and 91 mm/sec (215 ipm) WFS as constant process parameters. The arc current was measured during the weld when the laser was positioned to interact at various positions along the weld direction relative to the GMAW torch, including laser leading, lagging, and coincident with the GMAW torch. The positional measurements were obtained between the position at which the GMAW electrode extends to the surface, and the point laser beam focus spot. The results of the experiments are shown in Figure 3.

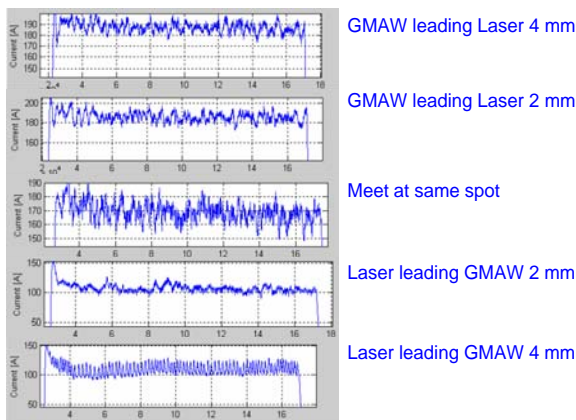


Figure 3: Affect of laser-to-arc spacing on arc current.

Note that although the positional measurements are taken between the point at which the extended wire would meet the work-piece, the arc will tend to take the path of least resistance to the work-piece, i.e. nearly straight down from the end of the electrode. This is an important fact to consider when evaluating the results. When the laser trailed the GMAW torch by the greatest amount, the current signal was at its maximum. It is likely the laser did not strongly interact with the arc in this case. When the laser led the electrode, it is conceivable that the increased penetration caused by the laser led to an increase in arc resistance resulting in the reduced current, as shown. The additional penetration associated with this condition may be the cause of the decrease in current. Additional explanations are presented in Travis *et al* [10, 11].

Thermal Modeling of Hybrid Welding

Objective

This portion of the paper focuses on the development of a thermal model for hybrid welding to calculate the temperature history of the part during the weld process. In the next phase of research, this temperature history will be used as input to an elasto-plastic finite element model in order to predict the effect of stress and the degree of distortion in structures that are welded by this method.

The heat source model outlined by Goldak *et al* is used to determine the effects of the thermal load in the laser-GMA Hybrid welding process [14]. First, a GMA welding model and a laser welding model are individually generated, and a Finite Element Model (FEM) simulation is executed to compare the effects of each process. Next a heat source model is generated for the Laser-GMA Hybrid process by directly combining the laser and arc heat source models through the concept of superposition.

The thermal model results are compared to experimental bead-on-plate fusion zone measurements for each welding process. The GMA welds were created using a constant voltage power supply set at 20 V, a wire feed rate of 84.7 mm/s (200 ipm), and using Ar-10% CO₂ shield gas flowing at 0.47 L/s (60 cfh). Note that the addition of metal via the weld wire to the weld plate was not considered in the thermal model; instead, a pre-placed bead cap was included in the model geometry. Autogenous laser welds were performed using a 14kW CO₂ continuous wave laser operating at a nominal power of 4 kW, with helium shield gas flowing at 1.57 L/s (200 cfh). The hybrid (GMA + laser) welds were performed using a direct combination of the aforementioned parameters.

Description-Modeling Approach

A reliable finite element model can serve as a useful tool in design and manufacture. The proposed model involves a three-dimensional transient thermal heat source model with free convection; however, no fluid flow or mass transfer is currently considered. The analysis is performed on half of a symmetric 150 × 150 × 5 mm plate possessing the material properties of ASTM 131 grade EH-36 steel. Thermal properties are assumed to be comparable to typical mild steel, having a melting point of approximately 1504°C [15]. The latent heat of fusion is a necessary parameter to account for the energy used to melt material in the fusion zone [16]. In order to achieve model convergence, a large range of latent heat was used as described by Sun *et al* [17]. Twenty node, hexagonal brick type elements were utilized to ensure reliable results, with six elements through the thickness of the material. Additional elements were added to the heat source zone to represent the crown of the weld. To achieve accurate results, setting the value for the time step duration

required careful attention. According to Goldak *et al*, in a standard three dimensional model sufficient results can be achieved by allowing the heat source to move half of the weld pool length in one time step [18]. Due to the comparatively large weld velocity employed in hybrid welding (16.93 mm/s or 40 ipm), for these experiments the heat source was only permitted to move one fifth of the weld pool length to ensure satisfactory results. The heat source was applied in the x direction along the back edge of the sectioned plate, as depicted in Figure 4.

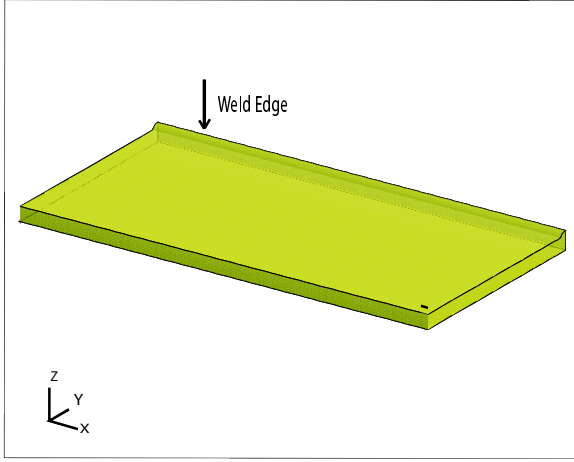


Figure 4: Depiction of thermal analysis plate.

A heat source having a double ellipsoidal power density distribution was used in the thermal model [14]. The heat source model is calibrated by adjusting the shape of the double ellipsoid through the semi-axes coefficients, a , b , and c_1 (or c_2), which correspond to the x , y , and z dimensions of the ellipses. Equation 1 and Equation 2 describe the distribution of heat over the front and rear quadrant.

$$q(x, y, z, t) = \frac{6\sqrt{3} f_f Q}{abc \pi \sqrt{\pi}} e^{\left[\frac{-3x^2}{a^2} - \frac{3y^2}{b^2} - \frac{3[z+v(\tau-t)]^2}{c_1^2} \right]} \quad (1)$$

$$q(x, y, z, t) = \frac{6\sqrt{3} f_r Q}{abc \pi \sqrt{\pi}} e^{\left[\frac{-3x^2}{a^2} - \frac{3y^2}{b^2} - \frac{3[z+v(\tau-t)]^2}{c_2^2} \right]} \quad (2)$$

The GMAW heat source power, Q , is calculated from the constant voltage set point, V , and current, I , measured from a Hall-Effect probe, as shown in Equation 3. Laser heat source power was determined through direct measurement. The process efficiency value, η , is determined from calorimetry experiments performed on GMA, laser, and GMA+laser hybrid welds [19].

$$Q = VI\eta \quad (3)$$

The entities f_f and f_r , in Equation 1 and Equation 2, determine the fractions of the heat source applied to the

front and rear quadrants of the weld respectively. A relationship exists between f_f and f_r , as seen in Equation 4 described by Goldak [14].

$$f_f + f_r = 2. \quad (4)$$

For our analysis f_f was given a value of 0.6, leaving f_r equal to 1.4.

A lag factor, τ , is used to describe the position of the source at time, t . The moving coordinate system is described by Equation 5.

$$\epsilon = z + v(\tau - t). \quad (5)$$

The quantity v is simply the welding velocity.

The geometry of the heat flux is set by the parameters a , b , and c_1 (or c_2) in Equation 1 and Equation 2 above. These parameters are weld specific, therefore they are dependent on the type of welding and welding conditions such as weld speed, current, voltage, and material properties.

Results

The equations described above were used to simulate the GMA, laser, and hybrid (GMA + Laser) welding processes. All models were applied to the EH-36 steel plate described above.

Figure 5 shows a GMA bead-on-plate weld made using the conditions in the *Arc Only* column of Table 1. The measured fusion zone width and depth are 2.9mm and 0.5mm, respectively. The fusion zone dimensions are used to verify the accuracy of the GMA thermal model results, shown in Figure 6. The fusion zone is taken to be the location of the liquidus isotherm ($T = 1504^\circ\text{C}$) at the center of the heat source. The modeled fusion zone width and depth are 2.7mm and 0.55mm, respectively. This result differs from experiment by 3% for the depth and 6% for the width of the fusion zone.

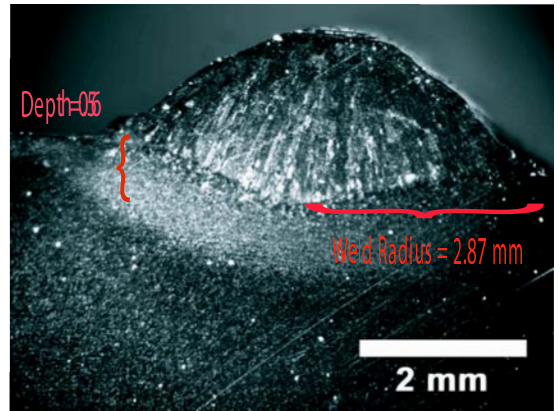


Figure 5: Micrograph of Arc Weld.

Figure 7 and Figure 8 compare the experimental and modeled cross sections for a laser beam weld. The model and

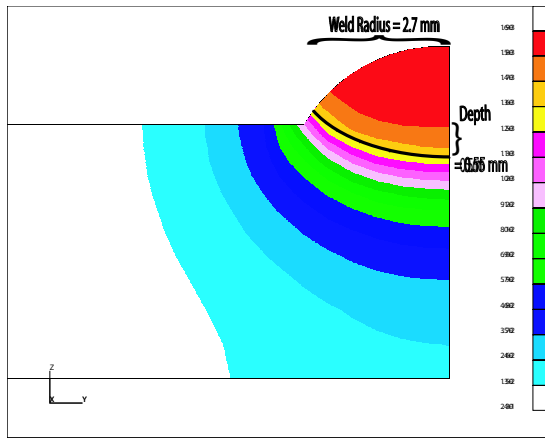


Figure 6: Cross Section of Arc Weld FEM.

	Arc Only / Arc Hybrid	Laser Only	Laser Hybrid
a	2.87 mm	0.5 mm	0.5 mm
b	0.56 mm	7.6 mm	18.6 mm
c1	2.87 mm	0.5 mm	0.5 mm
c2	11.48 mm	2.0 mm	2.0 mm
Power	—	4,000 W	4,000 W
Voltage	20 V	—	—
Current	165 A	—	—
η	73%	76%	76%
Velocity	16.9 mm/s	16.9 mm/s	16.9 mm/s

Table 1: Modeled and Experimental Weld Parameters

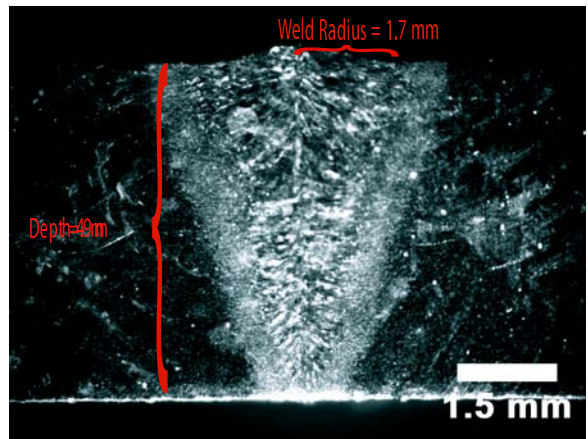


Figure 7: Micrograph of Laser Weld.

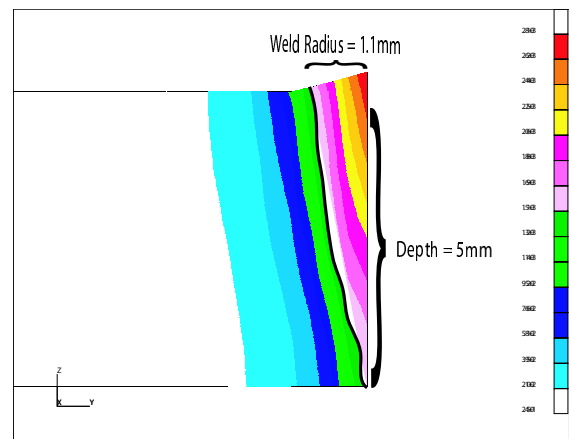


Figure 8: Cross Section of Laser Weld.

experimental parameters are shown in the *Laser Only* column of Table 1. In the experimental laser weld, full penetration of the 5 mm thick plate was achieved. The calibrated model results are in agreement; however, the fusion zone width in the modeled result is 35% greater than in the experiment.

The direct combination of the model parameters for the arc and laser did not yield acceptable results, and so the parameter, *b*, required slight modification. With the reformulated hybrid model, the predicted welding penetration depth was quite near the measured value, resulting in an error of only 1%. Similarly for the weld radius, an error of 9% can be seen in Figure 9 and Figure 10 below. The heat source model parameters used can be seen in the *Arc Hybrid* and *Laser Hybrid* columns of Table 1.

Future Work

Additional refinements will be made to the models above. Fluid flow and mass transfer are two areas to be explored in the future to improve the 3-D results. The models in the future also plan to use the calculated temperature history to investigate the stress and distortion associated with Laser-GMA Hybrid welding processes.

Summary

A variety of experiments have been undertaken to help better understand hybrid laser-GMA welding. Monitoring of arc current is strong to strongly correlate to variations in many process parameters. Special joint parameters enable single-pass hybrid welding of thick sections normally requiring multiple passes. A finite element model was generated to accurately display the temperature history in a hybrid welding process.

Acknowledgments

The authors would like to thank Mr. Jay Tressler for his patience, dedication, and laser welding experience in performing these numerous welds under difficult schedule constraints. We would also like to thank Dr. Geoffrey Dearden and Mr. Daniel Travis from the Laser Group at the University of Liverpool for their contributions to this work.

A portion of this material is based upon work supported by the Office of Naval Research through the Naval Sea

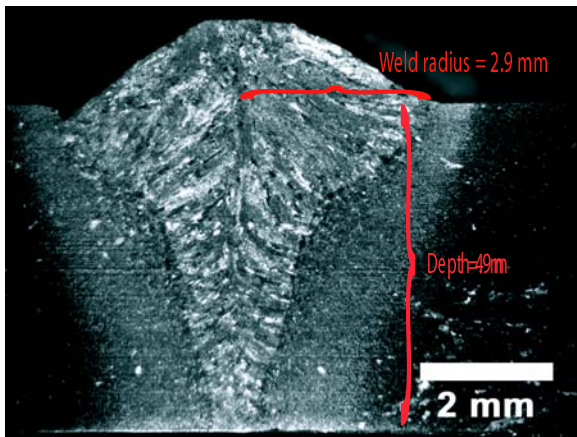


Figure 9: Micrograph of Hybrid Weld.

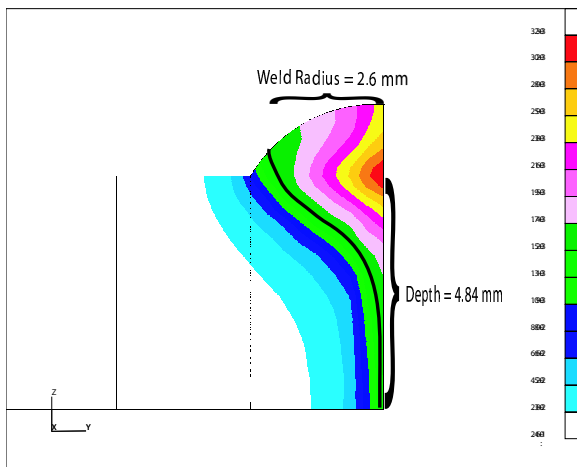


Figure 10: Cross Section of Hybrid Weld.

Systems Command under contract No. N00024-02-D-6604, Delivery Order No. 0019. Any opinions, findings, conclusions, or recommendations expressed in this material are those of the authors and do not necessarily reflect views of Office of Naval Research or the Naval Sea Systems Command.

References

[1] W.M. Steen and M. Eboo. Arc augmented laser welding. *Constr. III*, 7:332–336, 1979.

[2] W.M. Steen. Arc augmented laser processing of materials. *Journal of Applied Physics*, 51(11):5636–5641, 1980.

[3] H. Engstrom, K. Nilsson, and J. Flinkfeldt. Laser hybrid welding of high strength steels. In *Proceedings of the 2001 International Congress on Lasers and Electro-Optics (ICALEO 2001)*, number 303, 2001.

[4] C. Walz, T. Seefeld, and G. Sepold. Process stability and design of seam geometry during hybrid welding. In

Proceedings of the 2001 International Congress on Lasers and Electro-Optics (ICALEO 2001), number 305, 2001.

[5] W.W. Duley. *Laser Welding*. John Wiley, New York, 1999.

[6] Allen Sun, Jr. Elijah Kannatey-Asibu, and Mark Gartner. Sensor systems for real-time monitoring of laser weld quality. *Journal of Laser Applications*, 11(4):153–168, 1999.

[7] G. Dearden. Diagnostics in laser welding. Lecture Notes, 2001.

[8] E.W. Reutzler, C.J. Einerson, J.A. Johnson, H.B. Smartt, T. Harmer, and K.L. Moore. Derivation and calibration of a gas metal arc welding dynamic droplet model. In *Trends in Welding Research, Proceedings of the 4th International Conference*, pages 377–384, 1995.

[9] H.B. Smartt, K.L. Kenney, J.A. Johnson, N.M. Carlson, D.E. Clark, P.L. Taylor, and E.W. Reutzler. *Method and Apparatus for Assessing Weld Quality*. United States Patent, No. 6,236,017, May 2001.

[10] D. Travis, G. Dearden, and R.P. Martukanitz J.F. Tressler K.G. Watkins, E.W. Reutzler. Sensing for monitoring of the laser-gmaw hybrid welding process. In *Proceedings of the 2004 International Congress on Lasers and Electro-Optics (ICALEO 2004)*, 2004.

[11] Daniel Travis. Process monitoring of laser-arc hybrid welding. Msc, University of Liverpool, 2003.

[12] P. Kinney and D. Farson. Optimization of an innovative hybrid welding process for structural fabrication. In *Proceedings of the 2003 International Congress on Lasers and Electro-Optics (ICALEO 2003)*, number 303, 2003.

[13] S. Uchiumi, J. Wang, S. Katayama, M. Mizutani, T. Hongu, and K. Fujii. Penetration and welding phenomena in yag laser-mig hybrid welding of aluminum alloy. In *Proceedings of the 2004 International Congress on Lasers and Electro-Optics (ICALEO 2004)*, pages 76–85, 2004.

[14] J.A. Goldak, A.P. Chakravarti, and M. Bibby. A new finite element model for welding heat sources. *Metallurgical Transactions*, 15B:299–305, 1984.

[15] The British Iron and Steel Research Association, editor. *Physical Constants of Some Commercial Steels at Elevated Temperatures*. Butterworths Scientific Publications, London, 1953.

[16] L. O. Raymond and J. Chipman. Thermodynamic Functions of Iron. *Transactions of the Metallurgical Society of AIME*, 239:630–633, 1967.

[17] J. Sun, P. Michaleris, P. Marugabandhu, and J. Nucciarone. Large scale computing in welding. application: Modeling welding distortion of the maglev beam. Sept. 2004.

[18] J.A. Goldak, M. Bibby, J.E. Moore, R. House, and B. Patel. Computer modeling of heat flow in welds. *Metallurgical Transactions B*, 17B:587–600, Sept. 1986.

[19] S.M. Kelly. Unpublished research. 2005.